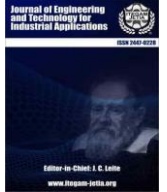




ISSN ONLINE: 2447-0228

ITEGAM-JETIA

Manaus, v.9 n.43, p. 64-70. Sept/Oct, 2023
DOI: <https://doi.org/10.5935/jetia.v9i43.910>



RESEARCH ARTICLE

OPEN ACCESS

MICROSTRUCTURAL CHARACTERIZATION OF FRICTION STIR WELDED AA5083 ALUMINUM ALLOY JOINTS

Kathiresan G.*¹, Rangunathan S.² and Prabakaran M. P.³

^{1,2} Varuvan Vadivelan Institute of Technology - Dharmapuri, Tamil Nadu, India.

³ Erode Sengunthar Engineering College - Erode -Tamil Nadu, India.

¹ <http://orcid.org/0000-0002-6428-4482> , ² <http://orcid.org/0009-0001-5234-6156> , ³ <http://orcid.org/0000-0002-4953-8528> 

Email: *kathirmechengg1980@gmail.com, ragusubramaniyan@gmail.com, prabakaranmp89@gmail.com

ARTICLE INFO

Article History

Received: September 30th, 2023

Revised: October 23th, 2023

Accepted: October 26th, 2023

Published: October 31th, 2023

Keywords:

Optimization,
Strength,
Hardness,
Chemical Analysis,
ANOVA.

ABSTRACT

The objective of the current work is to apply Taguchi L9 orthogonal array to enhance the welding process factors for friction stir welding (FSW) of AA5083 aluminium alloy plates. Using a randomized procedure, the Taguchi orthogonal array was implemented to identify the FSW process parameters such as the rotating speed of the tool, welding speed, and tilting angle of the tool. The optimum welding parameters for the ultimate tensile strength and hardness of the joints were predicted and the individual rank of each process parameter on the ultimate tensile strength and hardness of the friction stir weld was assessed by investigative ANOVA results and the S/N ratio (signal-to-noise ratio). The most desirable rotational speed of the tool, welding speed and tilting angle of the tool were 600 rev. per. min, 70 millimeter/min and 10° respectively for the ultimate tensile strength and 600 rev. per. min, 80 millimeter/min and 10° correspondingly for summit joint hardness. The outcomes of Analysis of Variance (ANOVA) designated that the tilting angle of the tool has the higher statistical effect succeeded by the welding velocity and rotational speed of the tool. Furthermore, metallurgical properties of the weld cross-sections were investigated by using optical microscope (OM), scanning electron microscope (SEM), energy dispersive spectroscopy (EDS) analysis. The microstructure of the stir zone reveals finer grain structure, directed to the higher hardness, which gives rise to higher tensile strength.



Copyright ©2023 by authors and Galileo Institute of Technology and Education of the Amazon (ITEGAM). This work is licensed under the Creative Commons Attribution International License (CC BY 4.0).

I. INTRODUCTION

Aluminum alloy AA 5083 is an Al-Mg based alloy that has many interesting properties such as structural material, moderately high strength, good corrosion resistance and low cost. These benefits are very attractive in the automobile industry and marine applications. Also, AA5083 is having light weight structures, high specific strength, good fracture toughness and excellent corrosion resistance. Traditional fusion procedures are used to join typical aluminium alloy joints, which have an impact on the weld joint's dispersion and encourage the formation of enhanced efficiency during the heat cycle [1, 2]. It is challenging to attain a sound welded joint due to the incidence of petrification fissures, scum enclosures and coarse grain porosities in the fusion welding of aluminum alloys [3]. Friction stir welding (FSW) has developed a technology of extensive attention because of its

several benefits, vital of which is its facility to weld otherwise unweldable alloys [4]. Compared with several of the fusion welding processes that are normally used for joining structural alloys, Friction Stir Welding is an emerging solid state joining method that avoids melting and recasting the material being joined [5].

II. THEORETICAL REFERENCE

The FSW process parameters are influenced by the mechanical and metallurgical properties of the welded joints [6]. Research has focused on examining how these factors, such as welding speed (mm/min), rotational speed of the tool (rpm), axial load (kN), tool geometry (like round, threaded, square, polygons etc.), tilting angle of the tool etc., affect the welded specimen's output characteristics to ascertain their separate influences [7, 8].

Taguchi statistical design is a powerful tool to identify significant factor from many by conducting relatively less number of experiments [9]. Furthermore, some authors aims to optimize the FSW process parameters of aluminum alloys using Taguchi orthogonal array technique [10]. Similarly, Kolraj et al. [11] studied the Taguchi method to optimization of FSW process parameters for joining of dissimilar AA2219 Al-Cu alloy and AA5083 Al-Mg alloy.

Shojaefard et al. [12] optimized the FSW process parameters with different pin profile, rotational speed, welding speed, tilt angle, shoulder diameter, pin diameter, shoulder concave angle and penetration depth by using Taguchi orthogonal array. Ravichandran et al [13] studied the role of FSW process parameters like welding speed, tool rotation speed, tool pin profile and shoulder diameter of tool on the output of elongation percentage and tensile strength of the joint. Kimura et al [14] examined the optimized process parameters during the AA5052 friction welding process.

The joint, which was in the perimeter softened area, had a joint efficiency of about 93% and broke in the base metal (BM). Geng et al. [15] optimized friction welding of aeronautic aluminum alloy 2024 joints. The optimized joint efficiency from Taguchi analysis reaches 92% of base metal and the fine recrystallized grains caused by the high temperature and plastic deformation are observed in the friction interface zone. During the FSW process, the material undergoes intense plastic decomposition at high temperatures, resulting in fine and balanced recrystallized grains [16, 17].

Excellent microstructure in friction stir welds creates good mechanical properties. In this study, Taguchi L9 Orthogonal Array (OA) method was used in order to optimize the mechanical properties of friction stir welding on AA5083 joint. After identified the optimum joint, tensile and hardness test were done to investigate the mechanical properties of the weld. The metallurgical properties were investigated with various sectors like Nugget Zone (NZ) Heat-Affected Zone (HAZ) and Thermo Mechanically Affected Zone (TMAZ) by using Optical Microscope (OM), Scanning Electron Microscopic (SEM) and Energy Dispersive X-Ray Spectroscopy (EDS) analysis. Furthermore, the microhardness survey was conducted across the weld zone to study the metallurgical effects of the friction stir weld joint.

III. MATERIALS AND METHODS

The present study was performed on AA5083 aluminium alloy with a thickness of 6 mm plates. The chemical composition and mechanical properties of the base metal AA5083 is given in Table 1 & Table 2. The AA5083 plates with dimensions of 120 mm×100 mm×6 mm were friction stir welded in the butt configuration using a vertical CNC milling machine. Welding was carried out on the butt joint structure using a friction stir welding machine. The butt joints were fabricated standard to the rolling direction. The experiments were performed using FSW process parameters of the designed L₉ OA.

The following FSW process parameters were used for joining of AA5083 like tool rotational speeds, tool welding speeds and Tool tilt angle (θ). The tools made of H13 grade tool steel with dimensions of pin length 5.70 mm, pin diameter 6 mm, tool shoulder 16 mm and shank 40 mm is shown in Fig.1. The pin is positioned at the center of the joint line and the welding tool is rotated clockwise direction during the joining process.

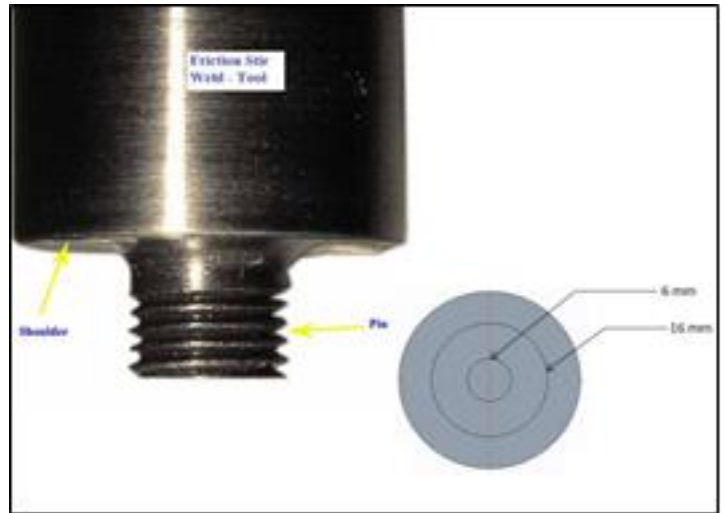


Figure 1: Friction Stir Welding Tool Specification.
Source: Authors, (2023).

The Taguchi method was used to optimize the welding parameters for friction stir welded AA5083 aluminium alloy for these investigations. In this method, the total degree of freedom (DOF), which can be computed by aggregating the individual DOF of each parameter, must be taken into consideration before selecting an appropriate orthogonal array.

Three levels were considered for each of the three process parameters for this experimentation. The levels of the each FSW process parameters were selected based on preceding literatures and given in Table 3. Hereafter, a L₉ orthogonal array with eight DOF was selected to assess how the welding parameters affect the final tensile strength and hardness of the joints.

Samples for tensile tests were prepared in accordance with ASTM E8 M-04 standard and the wire-cut Electrical Discharge Machining (EDM) was used to cut the smooth profile tensile specimens. The room-temperature tensile tests were conducted for all the samples on a universal tensile testing machine. Figure 5 shows tensile test samples of ASTM E8 M04 standard CAD model and FS welded AA5083 materials. Hardness test were conducted on weld nugget zone by using Vicker's microhardness machine. Microhardness tests samples were prepared according to ASTM standard and applied 0.5kgf with 10 seconds. The cross-sectioned samples were mounted in Bakelite, then ground and polished successively with diamond paste. The polished samples were etched with Keller's reagent for 25 s, and then analyzed optically for microstructural variations and possible flaws with a Nikon DIC microscope with a Clemex image analysis system. After fabricated FS welded specimens the SEM and EDX analysis were conducted.

Table 1: Chemical composition of AA5083 (Wt %).

Element	% (Percentage)
Silicon (Si)	0.14
Copper (Cu)	0.018
Ferrous (Fe)	0.30
Magnesium (Mg)	4.6
Chromium (Cr)	0.1
Titanium (Ti)	0.027
Zinc (Zn)	0.009
Manganese (Mn)	0.63
Aluminium (Al)	Bal

Source: Authors, (2023).

Table 2: Mechanical characteristics of AA5083.

Parent Material	AA5083
Ultimate Tensile Strength (MPa)	315
Yield Strength (MPa)	225
Percentage of Elongation (%)	15
Rigidity / Hardness (HV)	95

Source: Authors, (2023).

Table 3: Operational parameter – 3 Levels & 3 factors.

S.No	Operational Variables	Levels		
		1	2	3
1	Rotational Speed of the Tool (Rpm)	600	750	900
2	Welding Speed (mm/min)	70	85	100
3	Tilting Angle of the Tool (Θ)	0	1	2

Source: Authors, (2023).

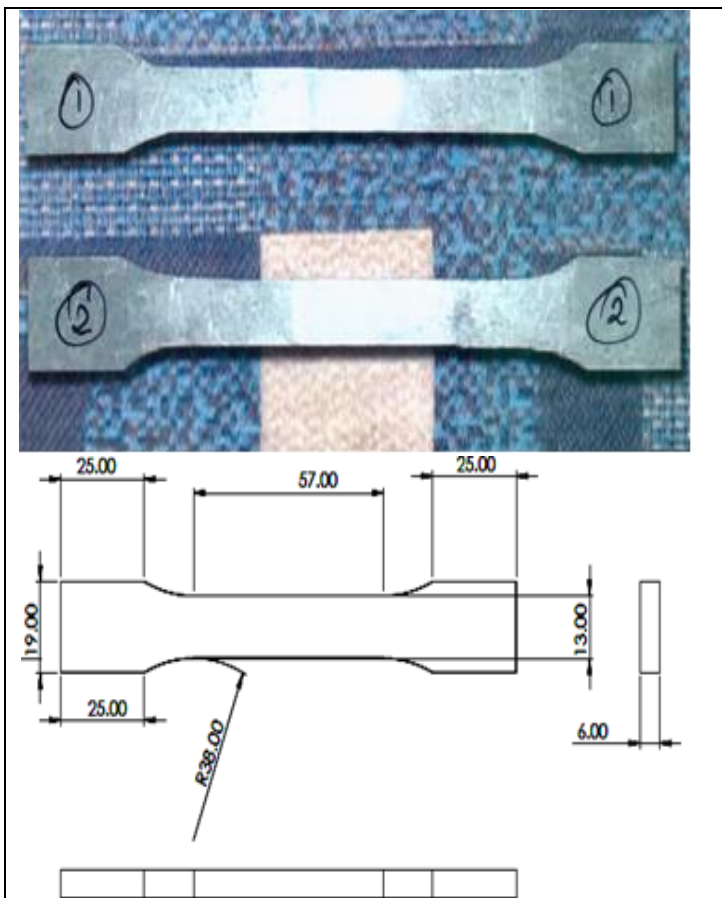


Figure 2: Tensile test specimens according to ASTM E8 M-04.

Source: Authors, (2023).

IV. RESULTS AND DISCUSSIONS

IV.1 SIGNAL TO NOISE (S/N) RATIO

The Signal to Noise (S/N) ratio is considered, based on the quality of the characteristics envisioned. The main aim designated in this study is maximization of the tensile strength and microhardness. Therefore, it is necessary to determine the higher and enhanced Signal-to-Noise ratio (S/N ratio). The tensile strength and microhardness of the nine test piece FSW joints values is considered to study the effects of the FSW process parameters given in Table 4. The experimental values of tensile strength and microhardness are converted into mean and SN ratio.

The calculated mean and S/N ratio values are tabulated in Table 5. The S/N ratio tensile strength and microhardness values of all levels are calculated and listed in Tables 6 and 7. The higher S/N ratio corresponds to the superior quality characteristics [18, 19]. The optimal level setting based on the S/N ratio values is R1S1T2 for tensile strength were obtained in Table 6. Based on S/N ratio values the optimal level setting is R1S2T2 for hardness were obtained in Table 7.

IV.2 ANALYSIS OF VARIANCE (ANOVA)

The purpose of ANOVA is to find a statistically significant factor. It gives a strong depiction as to exactly how distant the FSW process parameter affects the responses of tensile strength and hardness and the level of significance of the influence considered.

Table 4: Process parameters and their responses.

Trails	Rotational Speed of the Tool (RPM)	Welding Speed (mm/ min)	Tilting Angle of the Tool (Θ)	Tensile Strength (MPa)	Rigidity/ Hardness (Hv)
1	600	70	0	190.15	87
2	600	85	1	189.09	93
3	600	100	2	151.54	81
4	750	70	1	206.01	86
5	750	85	2	136.90	89
6	750	100	0	150.98	84
7	900	70	2	141.03	80
8	900	85	0	133.30	85
9	900	100	1	192.33	87

Source: Authors, (2023).

Table 5: Investigational Report with S/N ratio value.

Trails	Rotational Speed of the Tool (RPM)	Welding Speed (mm/ min)	Tilting Angle of the Tool (Θ)	Tensile Strength (MPa)	Rigidity/ Hardness (Hv)
1	600	70	0	45.58	38.79
2	600	85	1	45.53	39.36
3	600	100	2	43.61	38.16
4	750	70	1	46.27	38.69
5	750	85	2	42.72	38.98
6	750	100	0	43.57	38.48
7	900	70	2	42.98	38.06
8	900	85	0	42.49	38.58
9	900	100	1	45.68	38.79

Source: Authors, (2023).

Table 6: Response Table for S/N Ratios for Tensile strength.

Level	Rotational Speed of the Tool (RPM) (R)	Welding Speed (mm/min) (S)	Tilting angle of the Tool (Θ) (T)
1	44.91	44.95	43.89
2	44.19	43.59	45.83
3	43.72	44.29	43.11
Delta	1.19	1.36	2.72
Rank	3	2	1

Source: Authors, (2023).

Table 7: Response Table for S/N Ratios for Microhardness.

Level	Rotational Speed of the Tool (RPM) (R)	Welding Speed (mm/min) (S)	Tilting angle of the Tool (Θ) (T)
1	38.78	38.51	38.62
2	38.72	38.98	38.95
3	38.48	38.48	38.41
Delta	0.30	0.50	0.54
Rank	3	2	1

Source: Authors, (2023).

The ANOVA table for mean value of tensile strength and hardness are calculated and given in Table 8 and Table 9. Figures 3 and 4 depict the mean and S/N ratio main effects plots, respectively. Furthermore, the F-test termed after Fisher can also be used to determine which process has a significant effect on tensile strength and hardness.

The high F value indicates that the factor is highly significant in affecting the response of the process. In our investigation, tool tilt angle is a highly significant factor and plays a major role in affecting the tensile strength and hardness of the friction stir welded joints.



Figure 4.a: Means Plot.

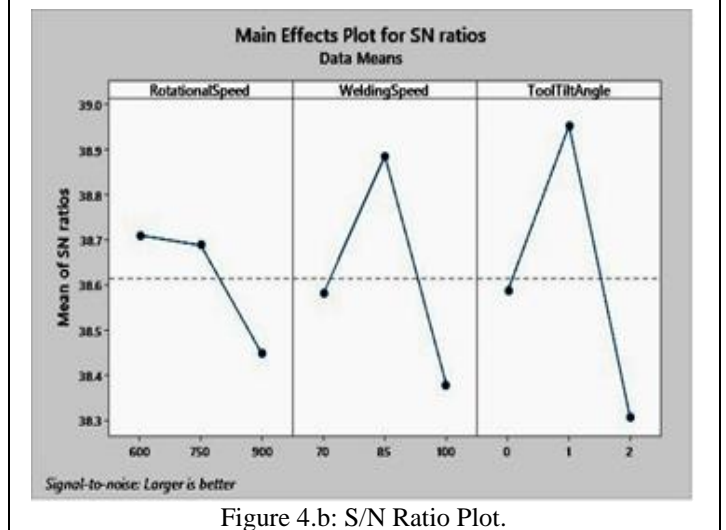


Figure 4.b: S/N Ratio Plot.

Figure 4.a & 4.b: Main effect plots on hardness.

Source: Authors, (2023).

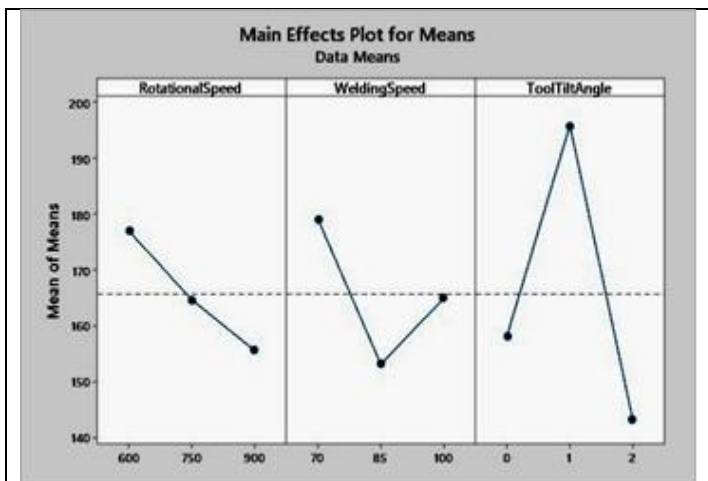


Figure 3.a: Means Plot.

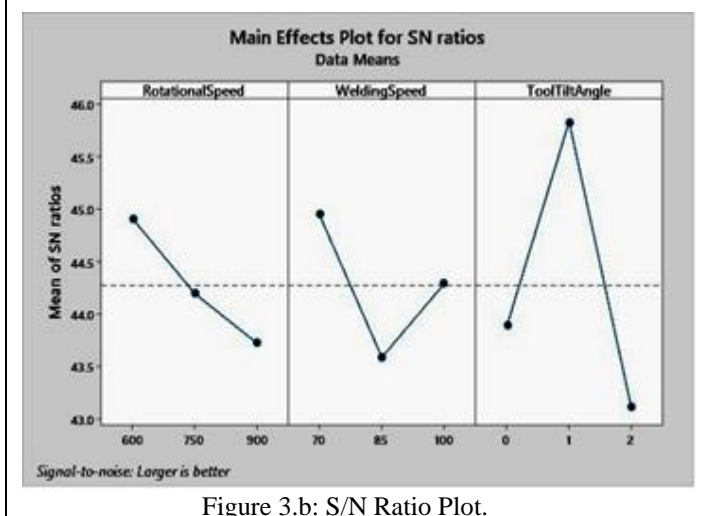


Figure 3.b: S/N Ratio Plot.

Figure 3.a & 3.b: Main effect plots on Tensile Strength.

Source: Authors, (2023).

Table 8: Analysis of Variance for tensile strength.

Source	DoF	Adjusted Sum of Squares	Adjusted Mean Squares	F Value	P Value	Percentage of contribution
Rotational Speed of the Tool (RPM) (R)	2	690.4	345.2	2.62	0.27	10.81
Welding Speed (mm/min) (S)	2	1014.0	507.0	3.84	0.20	15.88
Tilting angle of the Tool (Θ) (T)	2	4415.8	2207.9	16.74	0.05	69.17
Error	2	263.8	131.9			4.13
Total	8	6383.9				

Source: Authors, (2023).

Table 9: Analysis of Variance for hardness.

Source	DoF	Adjusted Sum of Squares	Adjusted Mean Squares	F Value	P Value	Percentage of contribution
Rotational Speed of the Tool (RPM) (R)	2	14.89	7.44	0.74	0.576	11.85
Welding Speed (mm/min) (S)	2	46.89	23.44	2.32	0.301	37.34
Tilting angle of the Tool (Θ) (T)	2	43.56	21.77	2.15	0.317	34.69
Error	2	20.22	10.11			16.10
Total	8	125.56				

Source: Authors, (2023).

Based on the experimentations, the optimum level setting was identified for the responses of tensile strength are R-1S-1T-2 and hardness is R-1S-2T-2. At certain levels of key parameters, the maximum value of ultimate tensile strength was projected. Significant FSW process parameters and their optimum levels have already been selected as rotational speed (level 1) of 600 rpm and Welding Speed (level 1) of 70 mm/min and tool tilt angle (level 2) 1 degree in Table 6.

Also, the optimum value of hardness was predicted at selected levels of significant parameters. Significant FSW process parameters and their optimum levels have already been selected as rotational speed (level 1) of 600 rpm and Welding Speed (level 1) of 85mm/min and tool tilt angle (level 2) 1 degree in Table 7. Confirmation tests were carried out with a cylindrical threaded pin profile and other process parameters were set at their predicted optimal levels. Three tensile and hardness specimens were subjected to tensile and hardness testes, and the average value of the friction stir welded AA5083 was 216 MPa and 97HV.

IV.3 MICROSTRUCTURE OF FRICTION STIR WELDED AA5083 OPTIMUM JOINT

The microstructure of the base metal and welded material was characterized using optical microscopy (OM) and scanning electron microscopy (SEM). The examined specimens cut from the transverse cross section of optimum weld were ground and polished according to the standard procedures and then etched with Keller's reagent for Observation. Fig.5 shows the microstructure of base metal AA5083 where Mg₂Si eutectic constituents in the same direction in primary aluminum solid solution.

This is affected by the effect of the shoulder of the tool, which is much wider than the tool itself. When it touches the plate, the shoulder produces a stirring effect, which spreads down into the plate. On the top side, a small ridge can be seen where the travel and the rotation directions of the shoulder coincide. Fig. 6 also shows the friction stir welded Thermo Mechanically Affected Zone (TMAZ) close to the nugget zone. Several Mg₂Si particles dissolved into the metal matrix, and the grains exhibit part recrystallization.

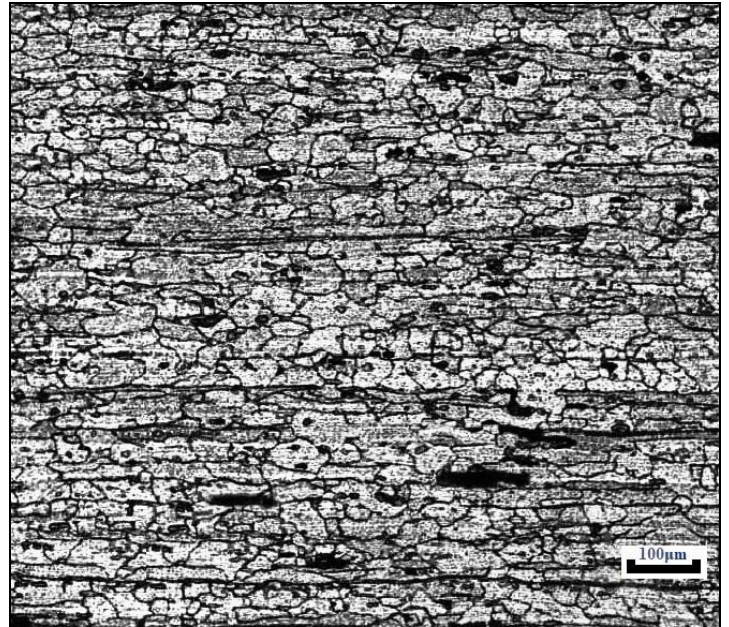


Figure 5: Microstructure of the base metal AA5083. Source: Authors, (2023).

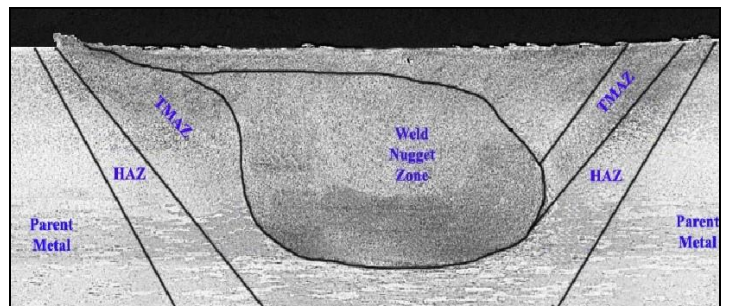


Figure 6: Microstructure of Friction Stir Welding Area of Metal AA5083. Source: Authors, (2023).

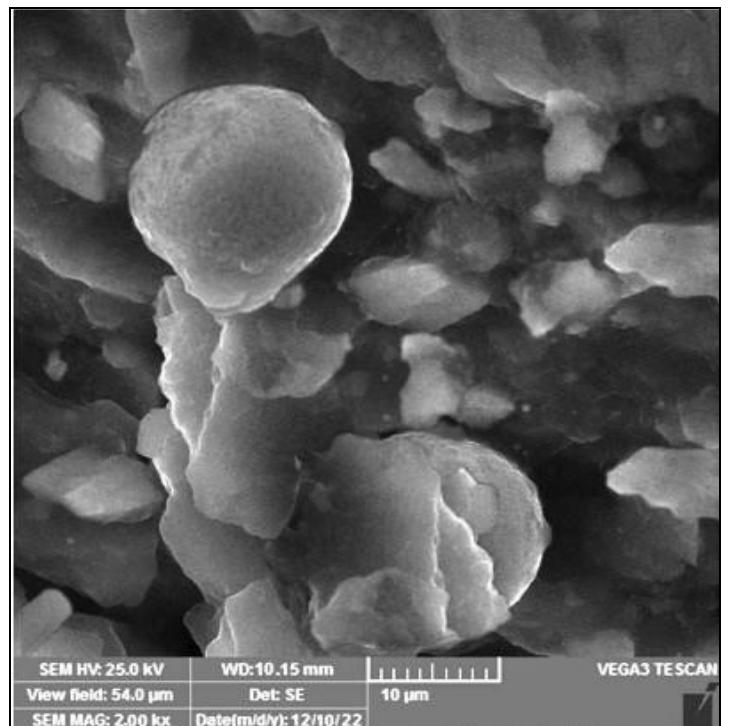


Figure 7: SEM Micrograph of Friction Stir WNZ. Source: Authors, (2023).

The microstructure shows the weld interface between AA5083 and the nugget zone with fusion line at the center. The fusion is complete without any discontinuities. The TMAZ revealed that some Mg₂Si particles had partially dissolved. The WNZ revealed Mg₂Si fragments in a matrix of aluminium as seen in Fig. 7. The agitation zone had significantly and equalized grains. This structure was produced by dynamic recrystallization and static grain growth after welding [20]. The micrographs were taken at the center and at the bottom of the nugget zone. The microstructure shows fine fragmented particles of eutectic Mg₂Si and the matrix undergone dynamic re-crystallization due to the rapid process of FSW with heat and stress. The assortments of particles were categorized by qualitative EDS (energy dispersive spectroscopy) analysis. The AA5083 has an Mg and Fe-rich phase or a multidimensional phase with Mg, Si and O₂-rich regions. They were noticed in the WNZ zone that was optimized. The other variations, such as Si and O₂ rich particles, were also seen. [21]. Tiny particles, which are primarily Mg and Si-rich, proved challenging to examine.

IV.4 MICROHARDNESS

The friction stir welded AA5083 alloy optimum joint were taken for the microhardness analysis. Microhardness test results are exposed in Fig.8 which demonstrates the hardness profile of the similar FSW'ed AA5083 Aluminum alloys at a rotational speed of tool 600 rpm, welding speed of 85 mm/min and tilting angle of the tool 1 degree. The meager microhardness levels found at TMAZ have been marked by the dotted lines. The base metal matrix that was not harmed had a 93 HV_{0.5} value, indicating that it was harder, and this pattern decreased as it moved towards the weld location. The minimum hardness value was found at TMAZ of 74 HV_{0.5} comparing with base metal and WNZ [22]. It can be noticed that the WNZ resulting higher hardness values than TMAZ where a maximum value of 83 HV_{0.5} was found at the optimum weld joint.

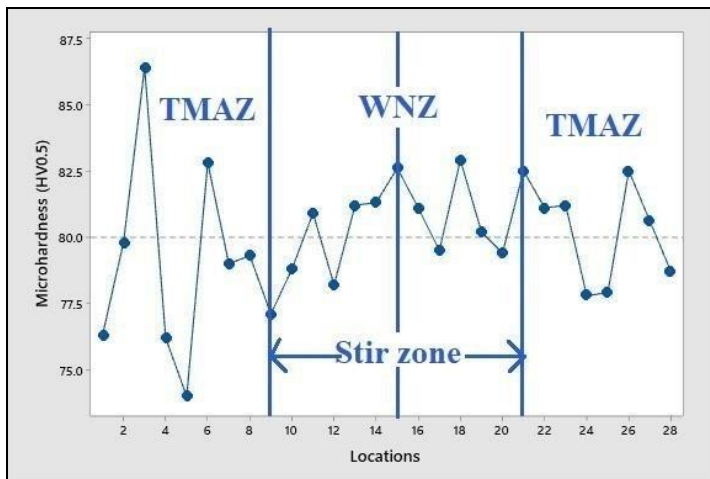


Figure 8: Microhardness analysis of FSW'ed Optimum Joint.
Source: Authors, (2023).

V. CONCLUSIONS

In this study, the welding process parameters of a Friction Stir welded AA5083 aluminium alloy have been optimized to maximize the tensile and hardness of the joints by using with Taguchi L₉ orthogonal array. The optimal combination of FSW parameters was a tool rotational speed of 600rpm, welding speed of 85 mm/min and tool tilt angle of 1 degree. The influence of

FSW process parameters was tool tilt angle followed by welding speed. The most significant process parameter was the tool tilt angle with a contribution of 69.17 percent. All fractures of the joints in the tensile testing occurred in the TMAZ near to the SZ. The finer grain size in the WNZ led to a higher hardness, which caused in greater fracture strength for the joints. The microstructure of the Welded Nugget Zone consists of tiny shredded eutectic Mg₂Si particles. The matrix had undergone re-crystallization due to the rapid process of FSW with heat and stress. Some Mg₂Si particles were dissolved into the metal matrix, and partial re-crystallization of the grains was perceived in the TMAZ. Successful microhardness testing revealed that, when compared to the base metals of AA5083 and WNZ, WNZ had a greater hardness value while TMAZ had a lower microhardness value.

VI. AUTHOR'S CONTRIBUTION

Conceptualization: Kathiresan G, Ragunathan S and Prabakaran M P.

Methodology: Kathiresan G and Prabakaran M P.

Investigation: Prabakaran M P.

Discussion of results: Kathiresan G and Prabakaran M P.

Writing – Original Draft: Kathiresan G.

Writing – Review and Editing: Prabakaran M P.

Resources: Ragunathan S.

Supervision: Ragunathan S.

Approval of the final text: Kathiresan G, Ragunathan S and Prabakaran M P.

VII. REFERENCES

- [1] E. Taban, E. Kaluc, "Microstructural and mechanical properties of double-sided MIG, TIG and friction stir welded 5083-H321 aluminium alloy", Kovove Materialy-Metallic Materials, vol. 44, pp.25-33, Jan. 2006.
- [2] S. Ji, R. Huang, X. Meng, L. Zhang, L. Y.Huang, "Enhancing friction stir weldability of 6061-T6 Al and AZ31B Mg alloys assisted by external non-rotational shoulder", Journal of Materials Engineering and Performance, vol. 26 pp.2359-2367, Mar. 2017.
- [3] A. Abdolazadeh, H. Omidvar, M.A. Safarkhanian, M. Bahrami, "Studying microstructure and mechanical properties of SiC-incorporated AZ31 joints fabricated through FSW: the effects of rotational and traveling speeds", The International Journal of Advanced Manufacturing Technology, Vol. 75, pp.1189-1196, Aug. 2014.
- [4] W B. Lee, Y.M Yeon, S.B. Jung, 2003) "The joint properties of dissimilar formed al alloys by friction stir welding according to the fixed location of materials", Scripta Materialia, vol. 49, no. 5, pp. 423-428, Sep. 2003.
- [5] Y. Li, L.E. Murr, J.C. McClure, "Flow visualization and residual microstructures associated with the friction-stir welding of 2024 aluminum to 6061 aluminum", Material Science and Engineering: A, vol. 271, no. 1-2, p.213-223, Nov. 1999.
- [6] H.M. Rao, B. Ghaffari, W. Yuan, J.B. Jordon, H. Badarinarayan, "Effect of process parameters on microstructure and mechanical behaviors of friction stir linear welded aluminum to magnesium", Materials Science and Engineering: A, vol. 651, no. 10, pp.27-36, Jan. 2016.
- [7] P. Cavaliere, "Friction stir welding of Al alloys: analysis of processing parameters affecting mechanical behavior", Procedia CIRP, vol. 11, pp. 139-144, Sep. 2013.
- [8] H. Khodaverdizadeh, A. Mahmoudi, A. Heidarzadeh, et al, "Effect of friction stir welding (FSW) parameters on strain hardening behavior of pure copper joints", Materials and Design, vol. 35, pp. 330-334, Mar. 2012.
- [9] N.D. Ghetiya, K.M. Patel and A.J Kavar, "Multi-objective optimization of FSW process parameters of aluminium alloy using Taguchi-based grey relational

analysis”, Transactions of the Indian Institute of Metals, vol. 69, no. 4, pp. 917-923, May. 2016.

[10] S. Kasman, “Multi-response optimization using the Taguchi-based grey relational analysis: A case study for dissimilar friction stir butt welding of AA6082-T6/AA5754-H111”, The International Journal of Advanced Manufacturing Technology, vol. 68, pp.795-804, Apr. 2013.

[11] M. Koilraj, V. Sundareswaran, S. Vijayan and S. Koteswara Rao, “Friction stir welding of dissimilar aluminum alloys AA2219 to AA5083 - optimization of process parameters using Taguchi technique”, Materials & Design, vol. 42, pp. 1-7, Dec. 2012.

[12] Mohammad Hasan Shojaeefard, Mostafa Akbari, Abolfazl Khalkhali, Parviz Asadi, Amir Hossein Parivar, “Optimization of microstructural and mechanical properties of friction stir welding using the cellular automaton and Taguchi method”, Materials & Design. vol. 64, pp.660-666, Dec. 2014.

[13] M. Ravichandran, M. Thirunavukkarasu, S. Sathish, et al, “Optimization of welding parameters to attain maximum strength in friction stir welded AA7075 joints”, Materials Testing, vol. 58, pp.206-210. Mar. 2016.

[14] M. Kimura, M. Choji, M. Kusaka, K. Seo, A. Fuji, “Effect of friction welding conditions on mechanical properties of A5052 aluminum alloy friction welded joint”, Journal of Science Technology of Welding and Joining, vol. 11, no. 2, pp. 209–215, Apr. 2006.

[15] Pei-hao Geng, Guo-liang Qin, Jun Zhou, Chang-an Li, “Parametric optimization and microstructural characterization of friction welded aeronautic aluminum alloy 2024”, Transactions of Nonferrous Metals Society of China, vol.29, no. 12, pp.2483-2495, Aug. 2019.

[16] B. Hari Babu and K. Madhivanan, “Experimental analysis of process parameters on friction stir welding of aluminium 6061 alloy”, International Journal of Advanced Research Trends in Engineering and Technology vol. 2, pp. 78-83, Oct. 2015.

[17] P. Cavaliere, A. De Santis, F. Panella, A. Squillace, “Effect of welding parameters on mechanical and microstructural properties of dissimilar AA6082-AA2024 joints produced by friction stir welding”, Materials and Design, vol. 30, pp.609-616, Mar. 2009.

[18] S. Vijayan, R. Raju, K. Subbaiah, N. Sridhar, S.R.K Rao, “Frictions stir welding of Al–Mg alloy-optimization of process parameters using Taguchi method”. Experimental Techniques, vol. 34, no. 5, pp. 37-44, Sep. 2010.

[19] S. Vijayan, R. Raju, S.R.K. Rao, “Multi-objective optimization of friction stir welding process parameters on aluminum alloy AA-5083 using Taguchi based grey relation analysis”, Materials and Manufacturing Processes, vol. 25, no. 11, pp. 1206-1212. Dec. 2010.

[20] K.V. Jata,S.L. Semiatin, “Continuous dynamic recrystallization during friction stir welding of high strength aluminum alloys”, Scripta Mater, vol. 43, pp.743-749. Sep. 2000.

[21] J. Gao, D.J. Quesnel, “Enhancement of the stress corrosion sensitivity of AA5083 by heat treatment”, Metallurgical and Materials Transactions A, vol. 42, pp.356-364, Feb. 2011.

[22] Z. Zhang, X. Yang, J. Zhang, G. Zhou, X. Xu, B. Zou, “Effect of welding parameters on microstructure and mechanical properties of friction stir spot welded 5052 aluminum alloy”, Materials and Design; vol. 32, pp. 4461-4470, Sep. 2011.